American Journal of Civil Engineering
2022; 10(3): 135-144
http://www.sciencepublishinggroup.com/j/ajce
doi: 10.11648/j.ajce.20221003.16
ISSN: 2330-8729 (Print); ISSN: 2330-8737 (Online)

Gel-bound Colourants as a Substitute for the Sprayed Application of pH-Indicator Solution

Nico Vogler*, Jens Lehmann, Tatjana Bohlmann, Jens Kronemann

Department 7 - Safety of Structures, Federal Institute for Materials Research and Testing (BAM), Berlin, Germany

Email address:

nico.vogler@bam.de (N. Vogler), jens.lehmann@bam.de (J. Lehmann), tatjana.bohlmann@bam.de (T. Bohlmann), jens.kronemann@gmx.de (J. Kronemann)

*Corresponding author

To cite this article:

Nico Vogler, Jens Lehmann, Tatjana Bohlmann, Jens Kronemann. Gel-bound Colourants as a Substitute for the Sprayed Application of pH-Indicator Solution. *American Journal of Civil Engineering*. Vol. 10, No. 3, 2022, pp. 135-144. doi: 10.11648/j.ajce.20221003.16

Received: May 16, 2022; **Accepted**: June 9, 2022; **Published**: June 27, 2022

Abstract: In general, pH-sensitive colorants such as phenolphthalein are applied on freshly split surfaces of building structures to determine the state of carbonation. For years, it has been known that the aerosols of phenolphthalein are suspected of being carcinogenic. Hence, more work has currently being done on alternative indicators for the use in research and the use on construction sites. Over the past years, mainly pH indicators from other research areas and natural dyes were investigated for their usability to cementitious systems. This paper presents the experimental results of using phenolphthalein solution bound in agar-agar gel. This gel-bound indicator allows the future use of the already known phenolphthalein dye without the health hazards for the user. To demonstrate the flexibility of the gel-bound colorant, different application forms of the indicator were carried out and assessed. In addition, the results obtained by the different methods were statistically evaluated to ensure validity. The accuracy of the results was confirmed by thermogravimetric analysis and IR spectroscopic studies as reference methods. It has also succeeded to demonstrate the comparability of the results achieved by the gel-bound colorant with the results of the common sprayed application method. As an additional gain in knowledge, comparative results of indicator tests, TGA analysis, and FTIR investigation are shown.

Keywords: Concrete Carbonation, Gel-bound Colorants, pH Indicator, Thermal Gravimetric Analysis, FTIR-ATR Measurements

1. Introduction

The steadily increasing share of CO_2 in the ambient air can already be observed for decades. The trends for the atmospheric CO_2 concentration have been published regularly by the National Oceanic and Atmospheric Administration since 1960 [1]. From these statistics, it is evident that the CO_2 concentration reached already values higher than 0.04% in ambient air and is further increasing [2]. It can be assumed that especially steel-reinforced concrete structures will be more affected in the future by these changing environmental conditions. One of the main issues is an interaction of the hardened cement paste with CO_2, or rather with carbonic acid. Carbonic acid is formed when CO_2 is dissolved in water (1). For example, Calcium hydroxide (2), single components of C-S-H (3), and ettringite (AFt) (4) become transformed into carbonates during this reaction.

$$CO_2 + H_2O \rightarrow H_2CO_3 \quad (1)$$

$$Ca(OH)_2 + H_2CO_3 \rightarrow CaCO_3 + 2H_2O \quad (2)$$

$$C_xS_yH_z + x\,H_2CO_3 \rightarrow CaCO_3 + SiO_2 \cdot y\,H_2O \quad (3)$$

$$3CaO \cdot Al_2O_3 \cdot 3CaSO_4 \cdot 32H_2O + 3H_2CO_3 \rightarrow 3CaCO_3 + 2Al(OH)_3 + 3CaSO_4 \cdot 2H_2O + 26H_2O \quad (4)$$

Thereby, various types of carbonates arise. A more detailed description of the carbonation processes taking place can be found in [3–10].

Besides structural changes, especially the decrease in the pH value has a significant impact on the durability of steel-reinforced concrete structures. The original high pH value of the hardened cement paste favors the formation of a 2 nm – 15 nm thick passivation layer. This layer protects the steel rebars against corrosion. Only when the pH value of the environment is higher than pH 9, the functionality of this layer is guaranteed [11]. Unfortunately, the pH value falls below pH 9 due to the carbonation process and the passivation layer gets unstable. Thus, the reinforcement is not protected anymore, and the corrosion is further in progress [12, 13]. To prevent corrosion, it is necessary to monitor the progress of carbonation regularly.

The most common method for the determination of the carbonation depth is sprayed application of Phenolphthalein solution. This method is regulated by the standards DIN EN 13295:2004-08, DIN CEN/TS 12390-10:2007-12, DIN EN 14630:2007-01 and prEN 12390-10:2017 [14-17]. Phenolphthalein is a pH-sensitive colorant. The molecular structure of the Phenolphthalein indicator changes depending on the environmental pH value. Thereby, the color alternates from colorless (< pH 8) to magenta (pH 8 – pH 12). However, it is presumed that the aerosols of phenolphthalein cause genetic defects, including cancer. Therefore, it is necessary to develop alternative technologies. In the last years, mainly pH indicators from other research areas and natural dyes were investigated for the application on cementitious systems [18-20].

For this research, an attempt was made to use a gel-bound phenolphthalein indicator for the determination of the carbonation depth. As carrier substance, agar-gel was used. The gel serves as a carrier framework within the phenolphthalein solution is held. This experimental setup allows an aerosol-free application of the phenolphthalein solution. The sprayed application of Phenolphthalein solution was used as the reference method. In addition, the thermogravimetric analysis (TGA) and the FTIR-ATR spectroscopy (Fourier Transform Infrared Spectroscopy in Attenuated Total Reflectance setup) were carried out. To obtain reliable results on the functionality of the gel-bound indicator, additional statistical evaluations were performed.

2. Gel-bound Indicator Solution

The principal idea of a gel-bound indicator is based on a rapid test for corrosion detection on stainless steel [21, 22]. The basic structure of the gel-bound indicator is the polysaccharide agar (-agar). It is obtained from red algae and consists of agarose (70%) and agaropectin (30%). The agarose molecules are responsible for gel-forming. At temperatures of 85°C – 95°C, the gelation of agar starts by forming disordered polymer coils. By subsequent cooling (to 33°C – 45°C) the single agarose coils start to join into a double helix structure by intramolecular hydrogen bonding (coil-helix transition) [23]. Additional water is stored within the double helix structure during this process. Thus, the structure becomes more stable. Finally, a three-dimensional gel matrix arises [24, 25]. The density of the arising polymer matrix depends on the amount of solved Agarose molecules. Up to 99% percent of this matrix may consist of water (H_2O). The slow release of the stored water (syneresis) supports the ion exchange of indicator and environment and favors agar as a carrier for pH-sensitive colorants.

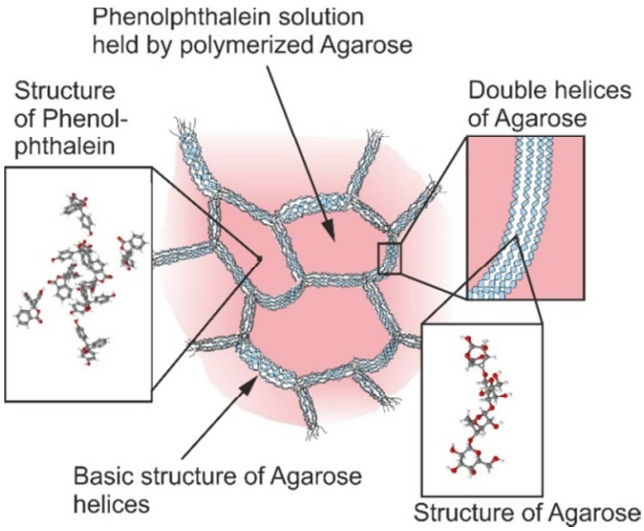

Figure 1. *Outlined structure of the gel-bound indicator solution.*

To obtain the gel-bound indicator, it is necessary to integrate the pH-sensitive colorant into the gel matrix. Therefore, the indicator must be kept between the bundled double helix structures (Figure 1). The simplest way to integrate the indicator into the matrix is to add the ready mixed phenolphthalein solution into the still liquid agar gel during the cooling process. The contained alcohol in the phenolphthalein solution causes a whitish discoloration of the gel-bound indicator. However, this discoloration improves the visibility of the later color change. For the preparation of the gel-bound indicator, the agar (3% by mass) was solved in heated H_2O. In the next step, a one-percent Phenolphthalein solution was added to the still liquid water-agar mixture. The mixture was filled in molds and cooled down. In a tightly sealed package, and stored under refrigerated conditions, the gel indicators are stable for several months without any loss in quality.

3. Materials and Methods

3.1. Specimen Preparation and Treatment

For the sample preparation, an Ordinary Portland Cement (Table 1) with a water/cement ratio (w/c) of 0.45 and a maximum aggregate grain size of 8 mm was used. The concrete specimens with sample sizes 100x100x600 mm were prepared by DIN EN 1766 [26]. After demolding, the specimens were cured for 28 days (d) underwater and stored for another 14 days in a 20°C and 65% relative humidity (RH) environment.

Table 1. *The composition of the cement types used, determined by using ICP-OES (inductively coupled plasma optical emission spectrometry).*

Cement type: CEM I 42,5 R	Mass%
CaO	64,28
SiO_2	19,62
Al_2O_3	4,6
Fe_2O_3	2,45
SO_3	2,59
MgO	2,22
K_2O	0,86
Na_2O	0,2
TiO_2	0,18

Before CO_2 treatment, the initial carbonation depth was determined accordingly to DIN EN 13295:2004-08 [14] in conjunction with DIN EN 14630:2007-01 [16]. Subsequently, the specimens were stored in a climate chamber with 1% CO_2 in ambient air, 21°C, and relative humidity of 60%. To obtain adequate carbonation depths, a treatment duration of 900 days was chosen. The storage of specimens under conditions with an artificially high CO_2 concentration is known as the accelerated carbonation method. It is a common procedure to obtain reliable results in a short trial period. During the treatment, the test specimens are exposed to a considerably higher CO_2 concentration compared to the natural CO_2 concentration. The effects and correlations between natural and accelerated carbonation conditions were already studied several times [6, 27, 28]. Sanjuan et al. [29] and Dhir et al. [30] have succeeded to find a correlation factor for a direct comparison of the different carbonation conditions. Also, the impact of curing, sheltering and CO_2 concentration, relative humidity, temperature, and other parameters were examined several times [3, 4, 7, 31, 32]. Accordingly, it can be assumed that the results obtained here are transferable to real environmental conditions.

3.2. Application of the Gel-bound Phenolphthalein Indicator

Figure 2. *Gel-bound indicator (a) pad shaped (b) bar-shaped (stick).*

The gel-bound indicator was used in two different ways. On the one hand, as a gel pad for fresh broken surfaces. On the other hand, shaped like a bar for the application in boreholes for the least possible damage to the building structure. To produce the gel pad, the liquid gel indicator solution was filled in a flat container and cooled down. This results in an indicator pad with a thickness of approximately 10 mm (Figure 2). The specimens previously stored in the CO_2 climate chamber were cracked just before the examinations. For the application, the pads were pressed on the fresh broken surfaces of the specimens. It was necessary to mark the dimensions of the specimen on the gel pad during the application. Only in this way, it was possible to determine the correct carbonation depth subsequently. After a duration time of three seconds, the indicator pads were removed from the surface. Afterward, the distance between the marked sample edge and the color change point was recognizable on the gel pad. Unfortunately, considerable damages to the building structure are unavoidable for the sprayed application of the indicator solution. Parts of the near-surface area of the building structure must be mechanically removed to generate the required fresh broken surface. The same applies to the removal of drilling cores from the building structure. The application of the indicator can also lead to color changes in the non-carbonated areas (high pH value) of the tested building structure.

For examinations with less impact on facades or other construction components, a bar-shaped gel bound indicator.

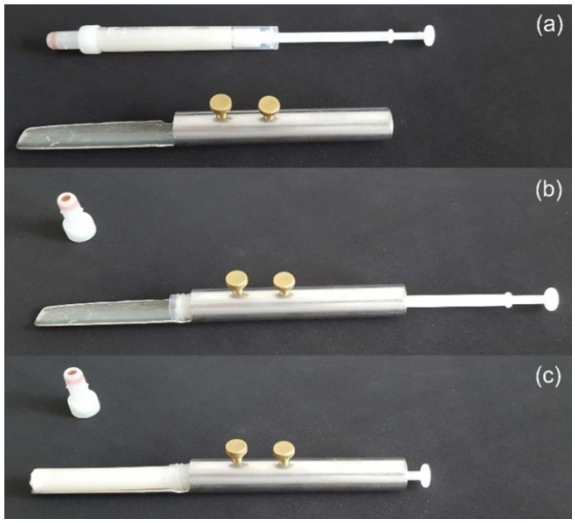

Figure 3. *Preparation of the indicator stick for minimally invasive application in concrete components (a) syringe filled with gel-bound indicator and tool for the application; (b) syringe inserted in the application tool, (c) fully prepared application tool for the gel-bound indicator test.*

was tested. For this application type, the liquid gel indicator solution was filled in syringes. After cooling down, a bar-shaped gel-bound indicator was obtained (Figure 2). For the application of the bar-shaped indicator, it was necessary to drill holes with a diameter of 16 mm into the specimen. The depth of the boreholes had to be at least in the same dimension as the concrete covering plus the width of the reinforcement. A considerable problem during the application was the resultant dust of the sample material in

the entire borehole. Thereby, the determined carbonation depth could be distorted. For this reason, an appropriate cleaning procedure was required. First, a major part of the powder was blown out by compressed air. In the next step, the hole was cleaned by injection of alcohol. Subsequently, the hole was blown out again by compressed air. For reaching the required cleanliness, the procedure was repeated at least two times for each borehole. Immediately after the cleaning procedure, the gel-bound indicator was applied inside the hole. For a duration time of a few seconds, the indicator stick was pressed against the walls of the borehole. A custom-made holder for the bar-shaped indicator was used to ensure a uniform pressure over the full length of the indicator stick inside the borehole (Figure 3). The color change was recognizable immediately after removing the indicator stick. Based on the distance between the upper edge of the indicator stick and the color change point, the carbonation depth could be determined.

3.3. Sprayed Application of the Phenolphthalein Solution

The specimens previously examined by the gel-bound indicators were also tested by the sprayed application of phenolphthalein solution. For this purpose, the specimens were cracked plane to the already existing boreholes. Subsequently, the fresh broken surfaces were treated with a solution of 1% Phenolphthalein solved in alcohol. After a duration time of 60 minutes, the carbonation depth was determined. Especially the surrounding areas of the former boreholes were considered. The analysis was performed accordingly to DIN EN 13295:2004-08 [14] in conjunction with DIN EN 14630:2007-01 [16].

3.4. Depth-Resolved Thermogravimetric Analysis and FTIR-ATR Spectroscopy

The carbonation depth was also determined by thermal gravimetric analysis and FTIR spectroscopy. With both methods, the available hydrate- and carbonate phases can be verified and distinguished. However, these technologies are rather unsuitable as standard determination methods for the carbonation depth. The considerable higher effort for the sample preparation and the longer measurement duration are major disadvantages for both methods. Nevertheless, due to the high information value, both methods were used as reference methods for this research.

To achieve a depth-resolved profile of the carbonation progress, complex sample preparation was required. Additional chemical reactions of the sample material during sample preparation had to be prevented. Especially, subsequent carbonation effects are critical. Also, interactions between the sample material and solvents used for the preparation should be avoided [33]. For the sample preparation, the specimen was cut into slices of 1.0 mm thickness. Subsequently, the slices were ground by hand with mortar and pestle. To prevent additional carbonation effects, all preparation steps were performed in isopropanol. In the end, the liquid phase was separated by vacuum filtration and the solid content was dried in a desiccator in an argon atmosphere [19, 34].

For thermal gravimetric analysis, the TGA/DSC 3+ Star System from Mettler Toledo was used. The sample material was heated up from 40°C to 1000°C with a heating rate of 10 K min^{-1}. All experiments were executed in a nitrogen atmosphere with a gas flow of 80 ml min^{-1}. For each measurement, 10 mg of sample material was filled in an Al_2O_3 crucible.

The Fourier transform infrared spectroscopy was carried out by using the attenuated total reflectance (ATR) method. Therefore, the Nicolet iS50 FTIR spectrometer from Thermofischer was used. The measurements were carried out in the wave number range between 4000 cm^{-1} and 400 cm^{-1} with a resolution of 4 cm^{-1}.

3.5. Statistical Evaluation

For better comparability of the different results, the Kolmogorov-Smirnov test and the Mann-Whitney U test were carried out. By using the Kolmogorov-Smirnov test, it is possible to analyze the individual results for a normal distribution. From this evaluation, it can be assumed whether enough individual measurement results were determined and a valid statement about the applicability of the gel-bound indicator is possible.

The Mann-Whitney U test is a non-parametric test for the evaluation of two independent samples for significant differences. This kind of test is necessary because the results of the different methods were not determined at the same points of the specimens. Therefore, possible sample-specific variations due to the inhomogeneous carbonation front must be included in the evaluation. Otherwise, differences in the results cannot be clearly attributed to the different application methods.

4. Results and Discussion

4.1. TGA/DTG and FTIR-ATR Spectroscopy

For the evaluation of the TGA results, the mass losses at the corresponding temperature ranges were determined. Due to the difficult distinction of the different levels of mass loss, the DTG curves (differentiated thermogravimetric curves) were also calculated. By combining the two signals, the individual mass loss of the different hydrate and carbonate phases could be quantified. Figure 4 shows the TGA and DTG curves summarized according to their depth arrangement in the specimen. For better clarity, only the curves that indicate significant differences in the mass losses are shown in the figures. By the DTG curves, it becomes apparent that carbonates (600°C to 700°C) are also verifiable in the core area (Ref) of the examined specimen. The low decomposition temperature suggests that these carbonates are attributed to the reaction of hydrates with the CO_2 in the ambient air. Natural carbonates, like calcite, normally decompose at temperatures higher than 700°C. Nevertheless, a clear connection between the carbonation effects and the sample preparation cannot be stated. However, due to the storage of the sample material in the desiccator (argon atmosphere) and the sample preparation

in isopropanol, this possibility can be largely excluded. Furthermore, it can be derived from the DTG curves that water released during the decomposition of $Ca(OH)_2$ (450°C) is also provable in the near-surface area. This area is considered as already carbonated. The cause for this signal is an encapsulation effect of the $Ca(OH)_2$ particles by a shell of $CaCO_3$. This effect is already described in more detail by Groves et al. [35], Vogler et al. [19, 34], Galan et al. [36], and Hidalgo et al. [37]. Due to the higher CO_2 content in the climate chamber, this effect can be observed more strongly during accelerated carbonation treatment. However, this effect is not detectable by performing the common phenolphthalein test. Especially when comparing the TGA results with the results of the indicator tests, this fact should be considered. In Figure 5 the mass losses calculated from the TGA curves are summarized. The major decrease of the $CaCO_3$ content (450°C to 750°C) is detectable to a depth of 18 mm to 20 mm. Below this area, the CO_2 content is almost constant at a level of 1%. The evidence of the hydrate phases proves more difficult. As can be taken from Figure 5, there is a large variation in the calculated values over the entire range. These variations are caused by an overlay of several effects. Molecular water, interlayer water of C-S-H, and water from the ettringite decomposition are released up to temperatures of approx. 200°C. In addition, water is formed during the carbonation of C-S-H and ettringite. The disturbing water can be reduced by additional drying processes. Nevertheless, it must be considered that the drying process can also affect the composition of the hydrate phases or lead to additional interactions [33]. The storage of the sample material in a desiccator in argon atmosphere is a very smooth drying method without major impact. The disadvantage of this method is a higher amount of remaining water and a more complex evaluation of the later results.

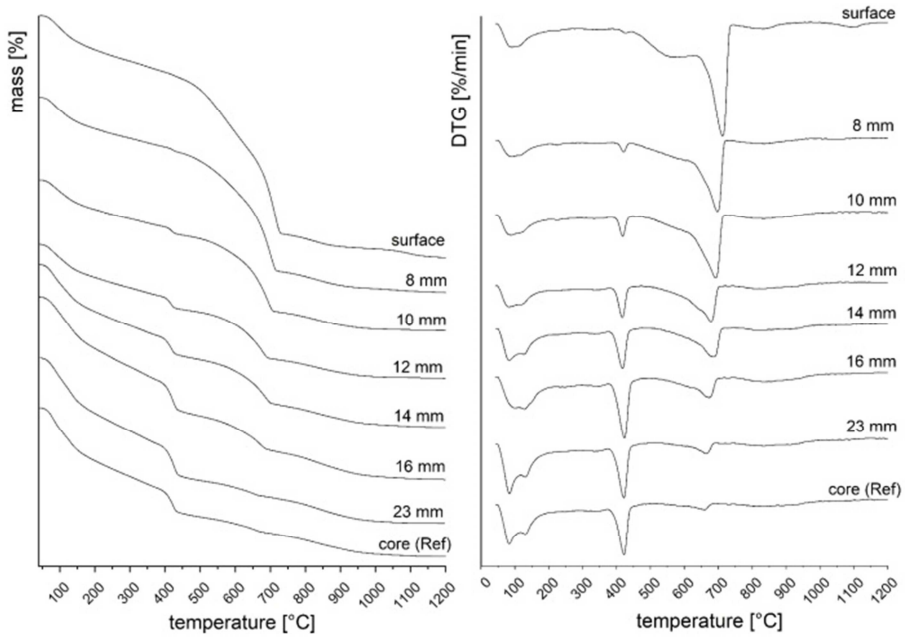

Figure 4. *TGA (left) and DTG (right) results of the depth-resolved thermalgravimetric analysis (data on the individual curves refer to the position in the test specimen.*

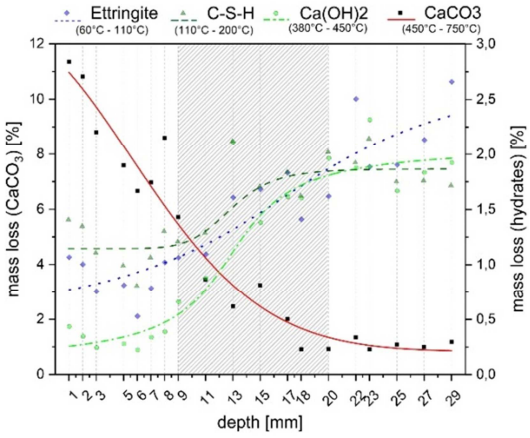

Figure 5. *Depth-resolved illustration of the mass losses based on the decomposition of hydrate and carbonate components determined by TGA.*

For all hydrate phases, it can be concluded (temperature range up to 450°C) that the relative mass loss is at a constant low level up to a depth of 8 mm to 9 mm. From about 9 mm depth, the mass loss in the temperature ranges up to 450°C increases significantly. It can be expected that the carbonation depth determined by the indicator test should be in the range between 9 mm and 18 mm. In areas below 18 mm to 20 mm, the content of C-S-H and $Ca(OH)_2$ is at a constant high level. In contrast, it seems that the ettringite content (60°C – 110°C) is further increasing in lower areas. The transition point between the steepest increase of the curve and the part that flattens out again was defined as the reference point for the determination of the carbonation depth.

Based on this point, a verifiable reaction depth of 20 mm to 22 mm for ettringite was determined. In the case of the C-S-H (110°C – 200°C) this point is at a depth of 15 mm to 17 mm.

The reaction range of $Ca(OH)_2$ (380°C - 450°C) is comparable to ettringite in a range between 20 mm and 23 mm.

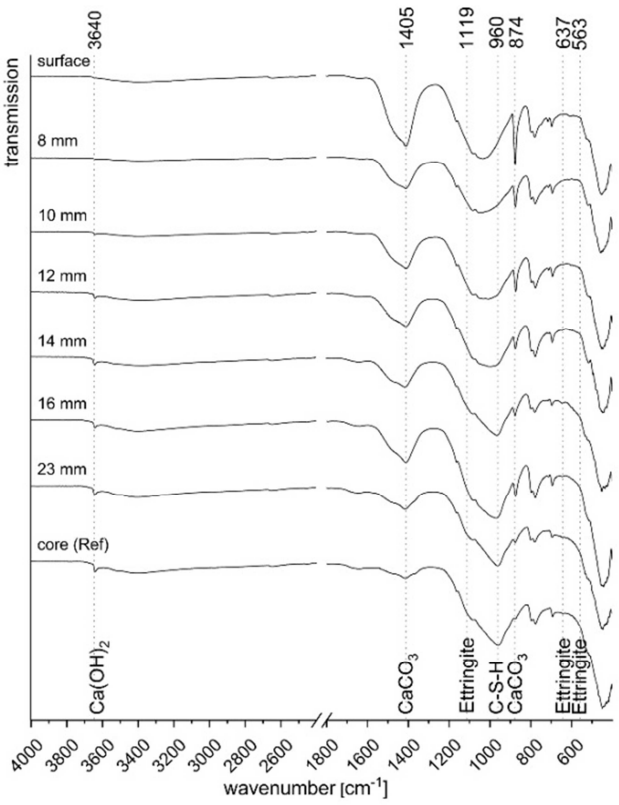

Figure 6. *Results of the depth resolved FTIR-ATR measurement, O-H stretching mode ($Ca(OH)_2$) {3640 cm^{-1}}, asymmetric C-O stretching mode ($CaCO_3$) {1405 cm^{-1}}, asymmetric S-O stretching mode (Ettringite) {1119 cm^{-1}}, asymmetric Si-O stretching mode (C-S-H) {960 cm^{-1}}, asymmetric O-C-O deformation mode ($CaCO_3$) {874 cm^{-1}}, Al-O-H bending mode (Ettringite) {637 cm^{-1}}, Al-O-H bending mode (Ettringite) {563 cm^{-1}}.*

The summarized results of the FTIR investigations are shown in Figure 6. In comparison to the TGA and DTG results the quartz from the aggregates is also detectable by FTIR analysis (1162 cm^{-1}, 1080 cm^{-1}, 798 cm^{-1}, 777 cm^{-1}, 693 cm^{-1} and 448 cm^{-1}) [38]. Furthermore, the typical vibrational modes of $Ca(OH)_2$ (3640 cm^{-1}) [39] and $CaCO_3$ (1405 cm^{-1}, 874 cm^{-1}) [40] can be found. In addition, ettringite (1119 cm^{-1}, 637 cm^{-1} and 563 cm^{-1}) [41, 42] and C-S-H (960 cm^{-1}) [43] has been proven. The vibrational modes of ettringite are only weak, or often overlaid by the vibrational modes of quartz, C-S-H, and $Ca(CO)_3$. The C-S-H is only verifiable based on a reflex at 960 cm^{-1}, which is also overlaid by the considerably wider Si-O oscillations of the quartz. All other vibrational modes of the C-S-H are completely overlaid and cannot be detected.

The Si-O stretching vibration of C-S-H at 960 cm^{-1} is detectable down to a depth of 14 mm. The Al-OH bending vibration at 637 cm^{-1} and the S-O stretching vibration at 1119 cm^{-1} of ettringite can be detected down to a depth of 12 mm. The Al-OH bending vibration of ettringite at 563 cm^{-1} is detectable down to a depth of 14 mm. The $Ca(OH)_2$ can be detected by the O-H stretching vibration at 3640 cm^{-1} down to the depth of 10 mm. Accordingly, it can be assumed that the sample material is completely carbonated down to the depth of 10 mm. This result agrees very well with the conclusions from the TGA results. The determination of the carbonation depth based on the increase of the $CaCO_3$ content proves difficult. This is caused by the circumstance that carbonates can be detected in the entire sample material, independent of the carbonation progress. This becomes evident by the thermogravimetric analysis (core (Ref): in the temperature range between 600°C and 700°C) as well as by the FTIR spectroscopy. The C-O stretching vibration at 1405 cm^{-1} and the O-C-O bending vibration at 874 cm-1 are detectable down to the core region of the investigated specimens. It can be assumed that the carbonates are already contained in the raw material. According to DIN EN 197-1 [44], up to 5% of minor components, such as carbonates, may be contained in the cement. It can also not be ruled out that the CO_2 entered the material during the sample preparation.

4.2. Application of the Gel Bound Indicator as a Pad

The initial trials with the entire gel pad (size: 125 mm x 125 mm) proved difficult. The required contact pressure could not be applied evenly to the entire surface. For further attempts, the pad was cut into strips with the dimensions of 20 mm by 50 mm. For the application, the pad strips were pressed against the fractured surface for about 3 seconds. At the same time, the gel pad strip was cut off at the outer edge of the tested specimen. After removing the gel pad from the surface, the carbonation depth was determined by measuring the distance between the color change point and the edge of the gel pad.

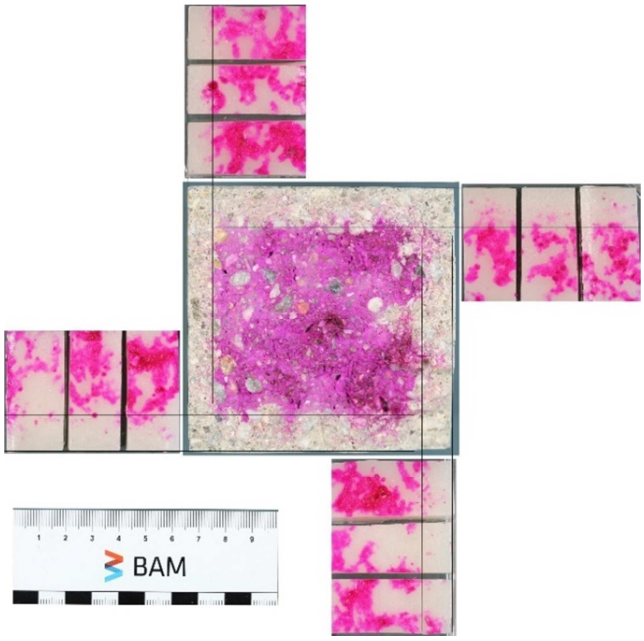

Figure 7. *Results of the gel-pad shaped indicator compared to the results of the sprayed application of phenolphthalein solution on a concrete specimen.*

The aggregates contained did not pose a problem in determining the carbonation depth. To obtain clear results,

three gel strips were applied at different locations on each side of the investigated fractured surface. The results of these tests are illustrated in Figure 7. For proving the functionality of the gel-bound indicator, the previously investigated surfaces were also treated by the sprayed application of the phenolphthalein solution. As can be seen in Figure 7, there is very good accordance between the results of the sprayed application and the application of the gel-bound indicator. It should be noted that the color change on the pad strip is the negative imprint of the specimen surface. However, due to the aggregate contained in the sample material, the repetition of the measurement is recommended.

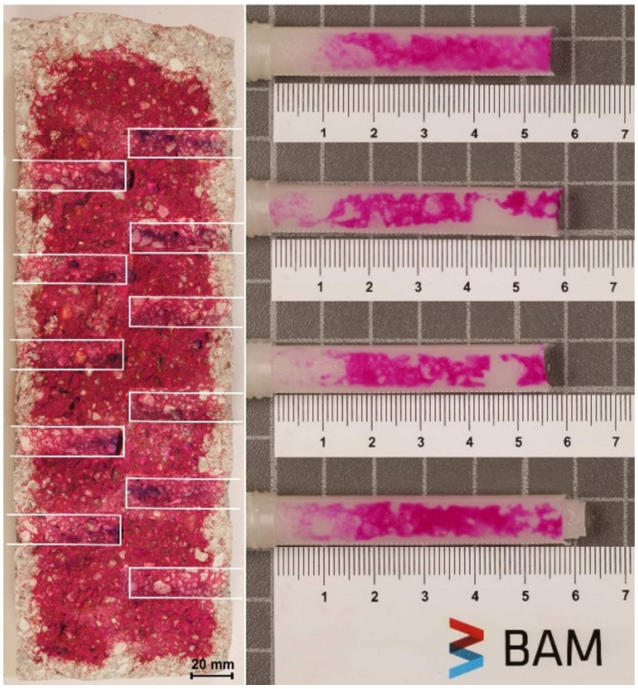

Figure 8. *Results of gel-bound indicator stick (right) compared to the results of the sprayed application of phenolphthalein solution on a concrete specimen.*

4.3. Application of the Gel Bound Indicator as a Stick in a Borehole

The results of the bar-shaped indicator match also very well with the results of the sprayed application method. There, the required cleaning procedure of the borehole plays a major role. As can be seen in Figure 8 (right side), there is a color change in the range which is considered as already carbonated. This is much weaker, but still recognizable. The reason for this effect is the drilling dust from non-carbonated areas. This had settled down on the inside of the entire borehole. However, with the previously described cleaning procedure, the drilling dust can be reduced to an acceptable level. During the application of the gel-bound indicator stick, it happened that no clear transition point was detectable. This was caused by the presence of aggregates. It has proven to repeat the measurement on another part of the sidewall of the borehole.

As already mentioned for the indicator pad, the sprayed application method was carried out afterward. To that, the specimens were split at the same level as the boreholes.

The fresh broken surfaces were treated subsequently with phenolphthalein solution (Figure 8 (left side)). Thereby, a less carbonation depth in the areas close to the boreholes (areas marked with the white lines) was found. This effect is related to the contamination with drilling dust from the non-carbonated areas. Apart from the application time, the delay between removing the gel-bound indicator and the determination of the carbonation depth has a significant influence on the result. After a wait of approximately two minutes, the optimal results were obtained. As can be taken from Figure 9, is the scattering of the individual results in the same range as the results of sprayed application method. A shorter wait led to lower carbonation depths due to the still available drilling dust. The faulty color change disappears within the first few minutes and the actual carbonation depth becomes visible. An increasing delay led to diffusion, or transport processes within the hydrogel and thus to a fading of the color change with faulty results. The first signs of this effect become apparent when edges and structures of the color change become blurred. This fading ensures considerable higher carbonation depths (Figure 9). Accordingly, comparable results to the sprayed application can only be achieved when the gel-bound indicator is used in the described way.

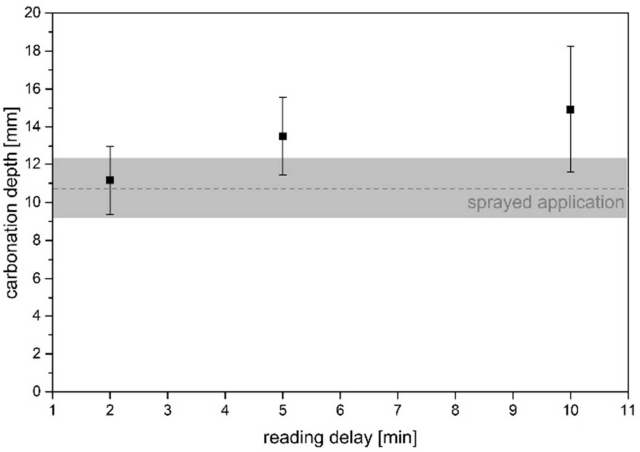

Figure 9. *Effect of the time delay between removing and reading the results from the gel-bound indicator compared to the results of the sprayed application of phenolphthalein solution by DIN EN 13295:2004-08.*

Chang et al. [45] attempted to correlate the results of the phenolphthalein test with the results of TGA, FTIR, and other methods. They found out that the color change point of phenolphthalein lies in a range between 50% and 100% of the completed carbonation process. Based on this assumption, the fully carbonated area should extend to a depth of about 8 mm to 13 mm.

Furthermore, Chang determined a ratio of 2.0 between the results of the phenolphthalein test and the results from TGA and FTIR. From the determined reaction depth of approx. 20 mm follows a carbonation depth of approx. 10 mm. Thus, both assumptions could be confirmed by the results obtained here.

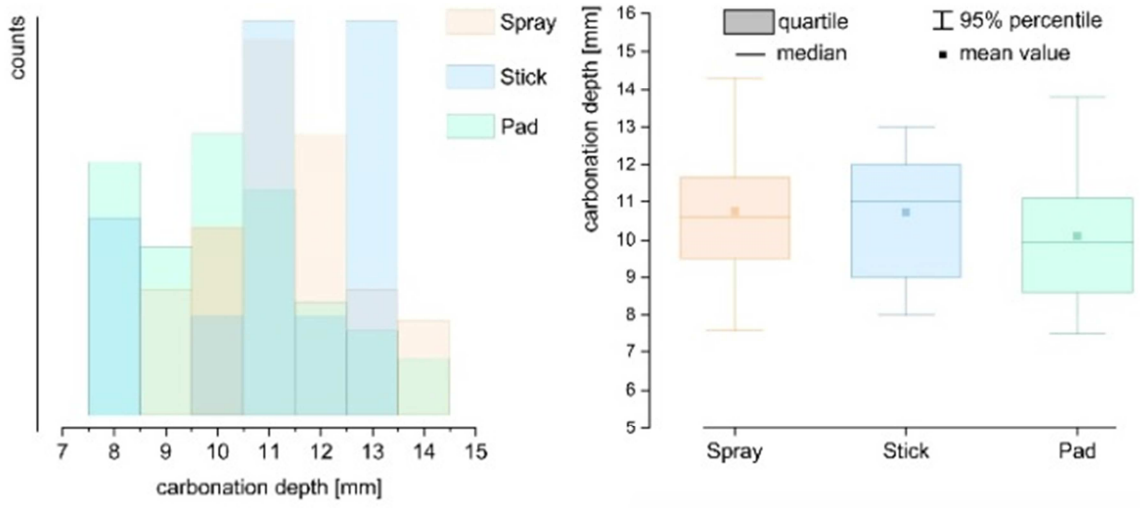

Figure 10. *Statistical evaluations of the carbonation depths were determined by the sprayed application of phenolphthalein solution (orange) minimal invasive application with the indicator stick (blue) and application of the pad-shaped gel-bound indicator (green).*

4.4. Statistical Evaluation of the Determined Carbonation Depth Results

For the implementation of the Kolmogorov-Smirnov test, the individual measurement results were sorted in ascending order of rank, for each of the three application methods. The cumulative distribution function was determined and compared with the corresponding hypothetical distribution. In the next step, the largest deviation within a measurement series was calculated. By the comparison with the critical values (significance level of 0.05), it was decided whether the corresponding null hypothesis had to be rejected or could not be rejected. The null hypothesis assumes that there are no significant deviations of the distribution function from the standard normal distribution. Hence, it can be concluded that the number of individual measurement results is sufficient. Only when this constraint is fulfilled, a valid statement on the functionality of the gel-bound indicators is possible. The Kolmogorov-Smirnov test did not reveal any significant deviations for the measurement series considered here. All values determined lay below the critical values for a significance level of 0.05 (Table 2). Thus, it can be assumed that there are enough individual measurement results for a valid conclusion.

To carry out the Mann-Whitney-U test, the results of the sprayed application method and the results of the gel-bound indicator were considered together. In the first step, the ranking of the individual measurement results was determined, and the respective rank sums were calculated. In addition, the corresponding U-values, mean values, and standard errors of the rank sums were determined. Based on these values, it was possible to calculate the Z-values. A comparison of the determined Z-values with the Z-score was finally used to decide whether the null hypothesis should be rejected or not.

The null hypothesis assumes that the individual results obtained here do not show any significant differences, regardless of the used method. When the null hypothesis cannot be rejected, a significant influence of the investigated sample material can be excluded with a 95% certainty. For the results considered here, it can be assumed that there is no significant influence of the sample material. Thus, the methods are reliable, and their applicability has been proven. A summary of the results can be found in Table 2.

Table 2. *Summary of the determined carbonation depths with the corresponding results of the statistical evaluation.*

	number of measurements	average carbonation depth	95% percentile range	interquartile range $Q_3 - Q_1$	Kolmogorow-Smirnow-test		Mann-Whitney-U-test	
					critical value	max. value	critical value	z-value
Spray	50	10.7 mm	7.6 mm -14.3 mm	9.5 mm - 11.7 mm	0,1923	0,0997	-	-
Stick	19	10,7 mm	8.0 mm - 13.0 mm	9.0 mm - 12.0 mm	0,3014	0,2022	Spray/Stick ±1,96	0,1112
Pad	48	10,1 mm	7.5 mm -13.8 mm	8.6 mm - 11.1 mm	0,2098	0,1608	Spray/Pad ±1,96	-1,0478

5. Conclusion

Within this research, it has been proven to show the functionality of gel-bound indicators as an alternative approach for the sprayed application of phenolphthalein solution. As a result of this work, it has succeeded to develop a functional method for determining the carbonation depth up to the patent stage [46]. The results obtained by the gel-bound indicators were in the same order of magnitude as the results of the sprayed application of phenolphthalein solution. The readability of the color change point was very good and

comparable for both gel-bound indicator applications. In contrast to the sprayed application, the time delay between removing the gel-pad indicator from the surface and the determination of the carbonation depth was only a few minutes. The color change of the phenolphthalein disappears continuously. After a few hours, it becomes completely disappeared. Thus, the storage of the used test kits is excluded, and immediate documentation of the results is required. The unused gel-bound indicators can be stored for several months in airtight packaging without any effect on the functionality. When using the indicator stick, special attention must be paid to the cleaning procedure of the borehole. Correct and valid results can only be achieved when the contamination by the drilling dust has been removed the best possible from the borehole previously. In addition, it should be noted that the aggregate contained in the concrete influences the scattering of the individual results. Therefore, the measurement must be repeated several times. For grain sizes larger than 32 mm, the number of individual measurements should be further increased. The comparability of the results obtained by the different application methods was also checked statistically. Neither an influence of the sample material on the results nor significant differences between the results of the different methods could be determined. In addition, it has been ensured that the number of measurements performed was sufficient to obtain statistically valid results.

The results of the indicator tests were also confirmed by thermogravimetric analysis and FTIR-ATR measurements. Both methods yielded consistent results regarding the carbonation behavior of the investigated samples. Due to the short measuring time, the FTIR-ATR measurement has proven as a very useful method. The carbonation depths estimated from the TGA and FTIR-ATR results agree very well with the results of the gel-bound indicator. When comparing the results of the indicator tests with the results of TGA or FTIR-ATR measurements, it should be noted that a direct comparison is only possible to a limited extent. This is caused by the fact that for the indicator test only the pH value of the pore solution is considered, while the analytical methods determine the composition of the sample material. However, by using the ratios determined by Chang et al. [45] it was possible to compare the analytical results with the results of the indicator tests.

Acknowledgements

The authors would like to thank all colleagues from the Federal Institute for Materials Research and Testing (BAM) for their support and input while executing this research.

References

[1] NOAA (National Oceanic and Atmospheric Administration), Earth System Research Laboratory, Trends in Atmospheric Carbon Dioxide. Available online: https://www.esrl.noaa.gov/gmd/ccgg/trends/ (accessed on 01.07.2021).

[2] Gapminder.com, Available online: https://www.gapminder.org/tools/#$state$time$value=2014;&marker$size$which=co2_emissions_tonnes_per_person&domainMin:null&domainMax:null&spaceRef:null;;;&chart-type=bubbles

[3] A. Leemann, F. Moro, Carbonation of concrete: the role of CO_2 concentration, relative humidity and CO_2 buffer capacity, Material and Structures (2017) 50: 30.

[4] A. Leemann, P. Nygaard, J. Kaufmann, R. Loser, Relation between carbonation resistance, mix design and exposure of mortar and concrete, Cement and Concrete Composition 62 (2015) 33-43.

[5] A. Morandeau, M. Thiéry, P. Dangla, Investigation of the carbonation mechanism of CH and C-S-H in terms of kinetics, microstructure changes and moisture properties, Cement and Concrete Research 56 (2014) 153-170.

[6] M. Fernández Bertos, S. J. R. Simons, C. D. Hills, P. J. Carey, A review of accelerated carbonation technology in the treatment of cement-based materials and sequestration of CO_2, Journal of Hazardous Materials B112 (2004) 193-205.

[7] S. O. Ekolu, A review on effects of curing, sheltering, and CO_2 concentration upon natural carbonation of concrete, Construction and Building Materials 127 (2016) 306-320.

[8] B. Šavija, M. Lukovic, Carbonation of cement paste: Understanding, challenges, and opportunities, Construction and Building Materials 117 (2016) 285-301.

[9] M. Castellote, L. Fernandez, C. Andrade, C. Alonso, Chemical changes and phase analysis of OPC pastes carbonated at different CO_2 concentrations, Materials and Structures 42 (2009) 515-525.

[10] H. Cui, W. Tang, W. Liu, Z. Dong, F. Xing, Experimental study on effects of CO_2 concentrations on concrete carbonation and diffusion mechanisms, Construction and Building Materials 93 (2015) 522-527.

[11] B. Beverskog, I. Puigdomenech, REVISED POURBAIX DIAGRAMs FOR IRON AT 25-300°C, Corrosion science Vol. 38 No. 12 (1996) 2121-2135.

[12] R. B. Figueira, Electrochemical Sensors for Monitoring the Corrosion Conditions of Reinforced Concrete Structures: A Review, Applied Science 7 (2017) 1157.

[13] M. Stefanoni, U. Angst, B. Elsener, Corrosion rate of carbon steel in carbonated concrete – A critical review, Cement and Concrete Composition 103 (2018) 35-48.

[14] DIN EN 13295:2004-08, Products and systems for the protection and repair of concrete structures – Test methods – Determination of resistance to carbonation (2004).

[15] DIN CEN/TS 12390-10:2007, Testing hardened concrete – Part 10: Determination of the relative carbonation resistance of concrete (2007).

[16] DIN EN 14630:2007-01, Products and systems for the protection and repair of concrete structures – Test methods – Determination of carbonation depth in hardened concrete by the phenolphthalein method (2007).

[17] E DIN EN 12390-10:2017-04, Testing hardened concrete – Part 10: Determination of the carbonation resistance of concrete at atmospheric levels of carbon dioxide; English version: prEN 12390-10: 2017.

[18] S. Chinchón-Payá, C. Andrade, S. Chinchón, Indicator of carbonation front in concrete as substitute to phenolphthalein, Cement and Concrete Research 82 (2016) 87-91.

[19] N. Vogler, M. Lindemann, P. Drabetzki, H.-C. Kühne, Alternative pH-indicators for determination of carbonation depth on cement-based concretes, Cement and Concrete Composites 109 (2020) 103565.

[20] T. Okonkwo, J. Nnaemeka, Hibiscus sabdariffa anthocyanidins: a potential two-colour end-point indicator in acid-base and complexometric titrations, International Journal of Pharmaceutical Sciences Review and Research Vol. 4 Issue 3 Article 021 (2010).

[21] J. Lehmann, A. Burkert and J. Mietz, Investigations proofing the passive layer stability of stainless steels, Materials and Corrosion, 67, No. 1 (2016).

[22] J. Lehmann, A. Burkert, U.-M. Steinhoff, German Patent Nr. DE 10 2010 037 775, (2014).

[23] K. Alba, V. Kontogiorgos, Seaweed Polysaccharides (Agar, Alginate Carrageenan), Encyclopedia of Food Chemistry. (pp. 240-250) Amsterdam, Netherlands: Elsevier. DOI: 10.1016/B978-0-08-100596-5.21587-4 (2018).

[24] V. Normand, D. L. Lootens, E. Amici, K. P. Plucknett, P. Aymard, New insight into agarose gel mechanical properties. Biomacromolecules 1 (2000) 730–738.

[25] S. J. Karcher, Molecular Biology - A Project Approach, Academic Press, ISBN 978-0-12-397720-5, (1995).

[26] DIN EN 1766, Products and systems for the protection and repair of concrete structures- Test methods- Reference concretes for testing (2017).

[27] M. Auroya, S. Poyeta, P. Le Bescopa, J.-M. Torrentib, T. Charpentierc, M. Moskurac, X. Bourbond, Comparison between natural and accelerated carbonation (3% CO_2): Impact on mineralogy, microstructure, water retention and cracking, Cement and Concrete Research 109 (2018) 64–80.

[28] N. Hyvert, A. Sellier, F. Duprat a, P. Rougeau, P. Francisco, Dependency of C–S–H carbonation rate on CO_2 pressure to explain transition from accelerated tests to natural carbonation, Cement and Concrete Research 40 (2010) 1582–1589.

[29] M. A. Sanjuan, C. Andrade, M. Cheyrezy, Concrete carbonation tests in natural and accelerated conditions, Advances in Cement Research 15-4 (2003) 171–180.

[30] R. K. Dhir, P. C. Hewlett, Y. N. Chan, Near-surface characteristics of concrete: prediction of carbonation resistance, Magazine of Concrete Research 41, No. 148 (1989) 137–143.

[31] D. Russell, P. A. M. Basheer, G. I. B. Rankin and A. E. Long, Effect of relative humidity and air permeability on prediction of the rate of carbonation of concrete, Structures & Buildings 146 Issue 3 (2001) 319-326.

[32] M. Elsalamawy, A. R. Mohamed, E. M. Kamal, The role of relative humidity and cement type on carbonation resistance of concrete, Alexandria Engineering Journal 58 (2019) 1257–1264.

[33] K. Scrivener, R. Snellings, B. Lothenbach, A Practical Guide to Microstructural Analysis of Cementitious Materials, CRC Press Taylor & Francis Group, ISBN 13:978-1-4987-3865-1, Boca Raton, (2016).

[34] N. Vogler, P. Drabetzki, M. Lindemann, H. C. Kühne, Description of the concrete carbonation process with adjusted depth resolved thermogravimetric analysis, Journal of Thermal Analysis and Calorimetry (2021). https://doi.org/10.1007/s10973-021-10966-1

[35] Groves GW, Brough A, Richardson IG, Dobsont CM. Progressive Changes in the Structure of Hardened C3S Cement Pastes due to Carbonation, Journal of the American Ceramic Society 74-11 (1991) 2891-2896.

[36] I. Galan, F. P. Glasser, D. Baza, C. Andrade, Assessment of the protective effect of carbonation on portlandite crystals, Cement and Concrete Research 74 (2015) 68-77.

[37] A. Hidalgo, C. Domingo, C. Garcia, S. Petit, C. Andrade, C. Alonso, Microstructural changes induced in Portland cement-based materials due to natural and supercritical carbonation, Journal of Materials Science 43 (2008), 3101-3111.

[38] K. Garbev, G. Beuchle, U. Schweike, D. Merz, O. Dregert, P. Stemmermann, Preparation of a Novel Cementitious Material from Hydrothermally Synthesized C–S–H Phases, Journal of the American Ceramic Society 97-7 (2014) 2298–2307.

[39] M. Chollet, M. Horgnies, Analyses of the surfaces of concrete by Raman and FT-IR spectroscopies: comparative study of hardened samples after demoulding and after organic post-treatment, Surface and Interface Analysis 43 (2011) 714–725.

[40] R. Ylmén, U. Jäglid, B. t-M. Steenari, I. Panas, Early hydration and setting of Portland cement monitored by IR, SEM and Vicat techniques, Cement and Concrete Research 39 (2009) 433–439.

[41] R. B. Perkins, C. D. Palmer, Solubility of ettringite ($Ca_6[Al(OH)_6]_2(SO_4)_3$ z $26H_2O$) at 5–75°C, Geochimica et Cosmochimica Acta Vol. 63 No. 13/14 (1999) 1969–1980.

[42] L. Yuke, Y. Zhengmao, W. Shuixan, X. Cheng, Influence of synthesis methods on ettringite dehydration, Journal of Thermal Analysis and Calorimetry 135 (2019) 2031–2038.

[43] I. García Lodeiro, D. E. Macphee, A. Palomo, A. Fernández-Jiménez, Effect of alkalis on fresh C–S–H gels. FTIR analysis, Cement and Concrete Research 39 (2009) 147–153.

[44] DIN EN 197-1:2011-11, Cement – Part 1: Composition, specifications and conformity criteria for common cements.

[45] C.-F. Chang, J.-W. Chen, The experimental investigation of concrete carbonation depth, Cement and Concrete Research 36 (2006) 1760–1767.

[46] J. Kronemann, N. Vogler, J. Lehmann, T. Bohlmann, German Patent Nr. DE 10 2017 100 746 (2017).